J Mater Sci: Mater Med (2010) 21:893–905
DOI 10.1007/s10856-009-3936-5

A porous scaffold for bone tissue engineering/45S5 Bioglass® derived porous scaffolds for co-culturing osteoblasts and endothelial cells

Sanjukta Deb · Ramin Mandegaran · Lucy Di Silvio

Received: 10 July 2009 / Accepted: 5 November 2009 / Published online: 29 November 2009

Abstract One of the major factors in the therapeutic success of bone tissue engineered scaffolds is the ability of the construct to vascularise post implantation. One of the approaches for improving vascularisation within scaffolds has been to co-culture human umbilical vein endothelial cells (HUVECS) with human osteoblasts (HOBS), which may then promote vascularisation and facilitate tissue regeneration. However, in order to mimic a natural physiological niche it is vital that the scaffold is able to support and promote the proliferation of both cell types and thus become a viable tissue engineered construct. In this study we report the development of a porous bioactive glass–ceramic construct and examine the interaction with human umbilical vein endothelial cells (HUVEC's) and human osteoblast-like cell both in mono and co-culture. The study clearly demonstrated that the scaffolds were able to support both endothelial and human osteoblast cell proliferation both in mono and co-culture. A comparison of the proliferation response of HUVEC and HOB in mono-culture on the test scaffolds and the commercial porous hydroxyapatite was assessed over a 28 day period (4, 7, 14, 21 and 28 days), using alamar Blue™ assay. Proliferation of HOB cells seeded in the scaffolds was consistently shown to be above those observed on commercial HA scaffolds.

S. Deb (✉) · R. Mandegaran · L. Di Silvio
Department of Biomaterials, Biomimetics and Biophotonics, King's College London Dental Institute, Floor 17, Tower Wing, Guy's Hospital, London Bridge, SE1 9RT London, UK
e-mail: sanjukta.deb@kcl.ac.uk

1 Introduction

Many approaches have been considered for tissue engineering however, all of them involve one or more of the key components namely: harvested cells, recombinant signalling molecules, and 3D scaffolds. The primary aim of bone tissue engineering is to replace diseased or damaged bone with a tissue engineered construct that is able to regenerate in vivo or in vitro. The scaffold is intended to replicate the functionality of the natural bone extracellular matrix (ECM). The ECM provides the microenvironment necessary for bone morphogenesis and thus, scaffolds designed to fulfil this role should closely mimic the in vivo environment for bone growth. The scaffold is ideally expected to function as a temporary ECM, capable of fulfilling the various biomechanical requirements, whilst being gradually resorbed and eventually replaced by host bone. The ability of the cells to fully migrate within the entire 3-D scaffold structure necessitates it to possess an interconnected porous architecture. The scaffold can play an additional role if the material used is osteoinductive, thus, not only allowing it to integrate with the host bone, but also assist it in bone healing. Consequently, a large number of materials such as polymers, glasses, glass–ceramics [1, 2] and composites have been explored as scaffold materials to function as substrates for cell seeding, however, vascularisation and functional integration with bone is yet to be achieved. Numerous studies have successfully demonstrated the ability to culture osteogenic cells (typically osteoblasts/osteoblast-like cells) singly on 3D porous scaffolds derived from various biomaterials in vitro. However, a loss in viability of the transferred cell mass is typically observed when such tissue engineered systems are transferred into an in vivo environment, ultimately resulting in poor bio-integration. The tissue

engineered systems typically fail in vivo due to slow capillary ingrowth, leading to cell hypoxia, death and implant failure. Thus, recent studies have focussed their attention in the development of vascularised tissue engineered constructs and 'pre-vascularised' constructs are being considered [3–6].

This study aimed to develop 45S5 Bioglass derived porous scaffolds and examine their ability to support in vitro cell populations of human osteoblasts (HOBs) and human umbilical vein endothelial cells (HUVECs) in monocultures and in co-culture with the long term aim of developing a prevascularised bone tissue engineered construct in vitro.

2 Materials and methods

2.1 Scaffold fabrication

Scaffolds were fabricated by mixing powdered 45S5 Bioglass® (particle size distribution 45–90 μm) with polyvinyl alcohol (PVA) (molecular weight: 33,000, Sigma-Aldrich) as the porogen. The glass-polymer mixtures were prepared using two weight ratios at 4:1 and 3:1 (weight/weight), respectively. The powder mix was spatulated in a ceramic pestle and mortar to ensure homogeneity of the mix. 0.7 g of the mixes were subsequently weighed and placed into a 12 mm diameter stainless steel cylindrical mould and compressed at 100 MPa yielding 12 mm diameter discs (green bodies) of both the 4:1 and 3:1 glass-polymer mixtures. A 9 h sintering process was performed, with a controlled 1.5 h 'ramping up phase', whereby the discs were heated from room temperature to 1000°C (rate of approx. 10.9°C min^{-1}) (CWF 11/5 furnace, Carbolite, Hope Valley, England) followed by a 'standing phase' of 3 h, where the temperature was kept constant at 1000°C. The discs were subsequently furnace-cooled to room temperature. The sintered scaffold discs derived from 4:1 and 3:1 glass-polymer compositions are here on referred to as BG1 and BG2, respectively.

2.2 Rhodamine dye infiltration

The BG1 and BG2 scaffolds were assumed to contain an interconnected porous network, which was tested by using a dye penetration technique. This was performed by addition of two drops of 1% aqueous rhodamine dye solution on the flat circular surfaces of BG1 and BG2 scaffolds. The scaffolds were cut in half, across the diameter and imaged under standard light microscopy (Meiji Techno, Tokyo, Japan) using a Nikon Coolpix 990 digital camera. The extent of dye infiltration throughout the thickness of the scaffold indicated the interconnectivity of the pores within the scaffolds.

2.3 Scanning electron microscopy

The BG1 and BG2 scaffolds were sectioned across the diameter and mounted on stubs (Hitachi, Hitachi High-Technologies, Wokingham, UK), gold sputter coated (E5100, Polaron Equipment Ltd., Hertfordshire, UK) and imaged by Scanning electron microscopy (SEM) (Hitachi S-3500 N, Hitachi High-Technologies, Wokingham, UK) in cross section, as well as, outer surface in order to determine an approximate value of the average pore size across the outer surface and inner structure of the scaffolds.

2.4 pH measurement and interaction of the scaffold with simulated body fluid

The pH of the immersion medium of the scaffolds was recorded over a 45 day period using a temperature-compensated pH electrode (Hydrus 100, Fisher Scientific, Loughborough, UK) by placing each scaffold in 3 ml of simulated body fluid (SBF). A comparison was performed using commercially available porous hydroxyapatite discs. Following each pH measurement, fresh SBF was added to the specimens. The interaction of the scaffolds with SBF produced according to the Kokubo recipe [7] was conducted with the experimental and HA scaffolds and then examined using FTIR and SEM. FTIR spectra were recorded for BG1 and BG2 scaffolds (i) prior to SBF immersion and (ii) after 46 days of SBF immersion (once scaffolds had been desiccated for 1 week to remove spectra interference by any residual water within the scaffolds). Spectra were collected in reflectance mode (PerkinElmer Spectrum One FT-IR Spectrometer) using a Diffuse Reflectance Sampling Accessory attachment. Spectra of SBF immersed scaffolds were subsequently compared to spectra of non-immersed scaffolds to determine whether functional groups associated with the formation of a bioactive HCA layer were present in SBF immersed scaffolds.

2.5 In vitro cytocompatibility studies

2.5.1 Primary human osteoblast (HOB) cell culture

A primary human osteoblast (HOB) cell model was used, briefly, cells were isolated from the femoral heads of patients undergoing surgery for total joint replacement, as described by Di Silvio et al. [8]. HOB cells were cultured in Dulbecco's modified Eagle's medium (DMEM), supplemented with 10% foetal calf serum (FCS), 1% non essential amino acids, L-ascorbic acid (0.150 g/l), 1% of 200 mM L-glutamine, 2% of 1 M HEPES, penicillin

(100 U/ml) and streptomycin (0.1 mg/ml) (All from Sigma, UK). HOBs were cultured at 37°C in a controlled humid atmosphere with 5% CO_2 .

2.5.2 *Primary human umbilical vein endothelial cell (HUVEC) culture*

HUVECs and all the associated products required for their subculture were purchased from Cascade Biologics Inc. (Mansfield, UK). Cells were cultured in Medium 200 supplemented with low serum growth supplement (LSGS) (Cascade Biologics Inc.), under standard conditions of a humidified atmosphere and at 37°C.

2.5.3 *Indirect MTT cytoxicity assay*

The *MTT* [3-(4,5-dimethyl-2-thiazolyl)-2,5-diphenyltetrazolium bromide] assay was used as an 'indirect' method to assess any potential cytotoxic leachables from BG1 to BG2 scaffolds. This quantifiable test measures cell metabolic function. If cells are exposed to toxic leachables the activity of the mitochondrial enzyme, succinate dehydrogenase is impaired. Sterile BG1 and BG2 scaffolds were placed in 3 ml of HOB medium (DMEM) for elution studies. The eluants (from each scaffold were collected at 24 and 72 h. The eluants were tested at 100, 90 and 50% concentration, with DMEM medium being used as the diluents (neat solution was diluted). Cells were exposed to the 24 and 72 h eluants from BG1 and BG2 for a period of 24 and 72 h The negative non-toxic control was DMEM and the positive toxic control was 10% industrial methylated spirit (IMS) (VWR International, Leicester). MTT (5 mg ml^{-1} diluted in DMEM phenol red-free medium) was added to the wells in an amount equivalent to 10% of the culture medium. Following 4 h incubation at 37°C, the medium was aspirated and the insoluble formazan salt produced was dissolved using 100 µl dimethyl sulfoxide (DMSO, Sigma D2650-tissue culture grade). The plates were gently agitated for 5 min to ensure complete crystal dissolution and optical densities were measured at a test wavelength 570 nm, subtracting background absorbance at reference wavelength 620 nm (Dynex Technologies, Chantilly, VA)

2.5.4 *Cell proliferation study (alamar Blue™)*

Proliferation of cells was determined using the alamarBlue™ assay (Life technologies) which is a redox indicator that measures proliferation quantitatively [9, 10]. As cells grow, there is an increase in metabolic activity giving rise to a reducing environment in the surrounding culture medium, whilst growth inhibition produces an oxidising environment. Reduction causes colour change of alamarBlue™ indicator from non-fluorescent (blue) to fluorescent (red). Proliferation studies of HOBs and HUVECs in monocultures and in co-culture were performed on BG1 and BG2 and commercial HA (100 µm average pore size SynHApor HA scaffolds, Hi-Por Ceramics Ltd., Sheffield, UK), as 3D porous control scaffold, experiments were performed in triplicate. Tissue culture plastic and medium supplemented with 10% IMS were used as 2D negative (non toxic) and positive (toxic) controls respectively. The test scaffolds were placed in a 24 well plate, cells were micro-seeded at a total density of 1×10^5 cells per scaffold (5×10^4 HOBs followed by 5×10^4 HUVECs per scaffold for co-culture). For HOB or HUVEC monoculture studies, a total of 1 ml primary HOB or HUVEC medium was added to each well, respectively. For co-culture studies, culture medium consisted of HOB and HUVEC medium in 1:1 ratio. Cells were cultured under standard conditions with the medium being replaced every 2–3 days.

Proliferation was measured on 4, 7, 14, 21 and 28 days post seeding as previously described [9, 10]. In brief, the medium was removed and replaced with 1 ml phenol red-free medium supplemented with 10% by volume filtered Alamar Blue™ stock solution (Serotec, Oxford, UK). After 4 h incubation in standard conditions, 100 µl aliquots from each of the three repeat wells for each test scaffold type was sequentially removed and added to wells in 96 well plates (eight replicates for each test scaffold) Absorbance was read on a fluorescent plate reader on emission wavelength of 590 nm (excitation wavelength 560 nm).

2.5.5 *Statistical analysis of MTT and alamar Blue™*

For the MTT assay, cytotoxicity of each scaffold eluant, at various dilutions, was compared to the negative control for each eluant and cell exposure time point. For each of the three cell conditions in the alamar Blue™ assay, cell proliferation in presence of each scaffold was compared to the negative control for each time point. Data was analysed using State ten statistical software. Significance was predetermined at $\alpha = 0.05$. The residuals following a one-way Anova of the data at each time point for both assays was not normally distributed, thus it was necessary to use a non-parametric Kruskal–Wallis analysis.

2.5.6 *Double cytotracker staining*

CellTracker™ Green CMFDA(5-chloromethylfluorescein diacetate) and CellTracker™ Orange CMRA (both Invitrogen, Paisley, UK) were used to selectively stain HUVECs and HOBs, respectively, prior to co-culture cell seeding of the scaffold. CellTracker™ dyes were selected as a means of distinguishing between different cell types in

3D co-culture using fluorescent microscopy allowing both cell types to be distinguished upon the same scaffold for up to 7 days under fluorescence—far longer than most other permanent cell dyes available [11]. The CellTracker™ reagents are taken up by viable cells and transformed by a glutathione *S*-transferase mediated reaction to form a cell-impermeant fluorescent dye-thioether conjugate, resulting in viable cells being visible under fluorescence [11]. The orange dye was diluted in serum-free DMEM (pre-warmed to 37°C) to form a working concentration of 30 μM. Culture medium was subsequently removed from each test scaffold and replaced with the 10 ml orange dye solution and further incubated for 45 min. Stock solution of green dye was diluted to a working concentration of 10 μM in serum-free HUVEC medium and the medium removed and replaced with the dye and incubated for 30 min. After the appropriate incubation time, the dye/culture medium solution was removed and replaced with normal culture medium and further incubated for 30 min. Cells were then trypsinized and microseeded onto duplicate BG1, BG2, and HA scaffolds in co-culture, at a total cell density of 1×10^5 (5×10^4 HOBs followed by 5×10^4 HUVECs) per scaffold/ml medium/well. 3 h post cell-seeding scaffolds were cut in half across the diameter of the flat surface (to determine cell infiltration into the scaffold in cross-section) and returned to their corresponding culture well. Scaffolds were viewed under fluorescence (548 nm absorbance and 576 nm emission wavelength for CellTracker™ Orange CMRA, 492 absorbance and 517 emission wavelength for CellTracker™ Green CMFDA) using a Leica SP2 confocal laser scanning inverted microscope (Leica Microsystems Inc., Mannheim, Germany) at ×10 magnification.

2.5.7 *Co-culture scanning electron microscopy*

HOBs and HUVECs were micro-seeded on the test scaffolds in co-culture in a 24-well plate at a cell density of 1×10^5 per scaffold as described previously. On day 3 post seeding, scaffolds were cut into half across the diameter of the flat surface. Culture medium was removed from each well and replaced with 1 ml of 10% neutral formalin buffer to fix the cells and the plate was kept in a refrigerator at 4°C until further processing. The formalin buffer was removed and samples sonicated for 1 h (1% osmium tetroxide in 0.1 M NaCacodylate buffer) and then washed in the NaCacodylate buffer (NCB) for 15 min, followed by a 1 h immersion in 1% tannic acid in 0.05 M NCB, after which the samples were washed in 0.1 M NCB for 20 min. Samples were then dehydrated using a series of ethanol dilution:, 10 min immersion in 20% ethanol, followed by 10 min at 30%, and so on up to 100% ethanol. After the 70% ethanol step, the series was interrupted by immersing the samples in 0.5 M uranyl acetate in 70% ethanol. Once sample dehydration was complete, the specimens were treated for 6 min in hexamethyldisilazane (HMDS) (Sigma) treatment and dried in air for 10 h. Samples were then mounted, gold sputter coated and viewed under SEM as described previously.

3 Results

3.1 Scaffolds and porosity

Porous discs of the sintered Bioglass scaffolds were obtained via the elimination of the polymeric porogen, PVA through a burn out process. The FTIR spectra confirmed that there was no residual PVA within the experimental scaffolds BG1 and BG2 as expected (Fig. 1) with no characteristic peaks for PVA evident (3290 cm^{-1} OH stretch; 2967 cm^{-1} CH_2 symm stretch; 1290 –OH in plane bending; 1100–1069 cm^{-1} –C–O– and –OH stretch). The interconnectivity of the pores within the scaffolds was examined by rhodamine dye infiltration, sections are shown in Fig. 2; the dye penetrated symmetrically through the 3D structure of both BG1 and BG2. This test only gave an indication of the interconnectivity, if the pores were not linked one would have expected to see a patchy appearance of the dye at the bottom end. The paler shades of the dye on the scaffold indicated dye adsorption relating to slower ingress, thus indicating the presence of narrower channels, whereas the dark red zones indicated the flow of the dye through wider channels and at no zone was there a total absence of the dye, thus suggesting interconnectivity. Furthermore, the SEM micrographs of both the scaffolds shown in Fig. 3a–d clearly showed a variability in the pore sizes and smaller pores were seen to exist within larger pores. No attempt was made to determine an average pore size as the aim was to create a scaffold with variable size pores with interconnectivity.

3.2 Interaction with SBF to determine the bioactivity and determination of pH in immersion fluids

BG1, BG2 and HA scaffolds were immersed in SBF and the pH measurements of the solutions for BG1, BG2 and HA is shown in Fig. 4. The pH of the SBF in which the BG scaffolds were immersed showed an initial increase after which, the pH of the SBF remained relatively stable at a slightly alkaline pH of 8.7 in SBF. HA immersion fluid showed a change in pH at day 2 after which a stable pH at an average of 7 was recorded.

The FTIR spectra of the scaffold BG1 before and after immersion in SBF shown in Fig. 5, revealed the presence of characteristic peaks associated with the formation of the

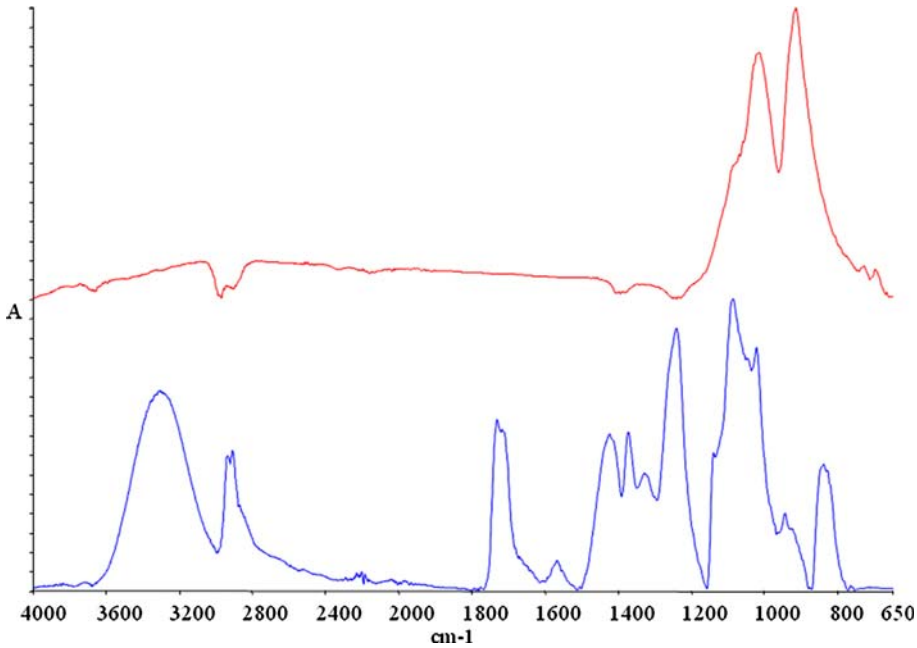

Fig. 1 FTIR spectrum of PVA (lower spectra) and the BG scaffold showing absence of PVA in the BG scaffold

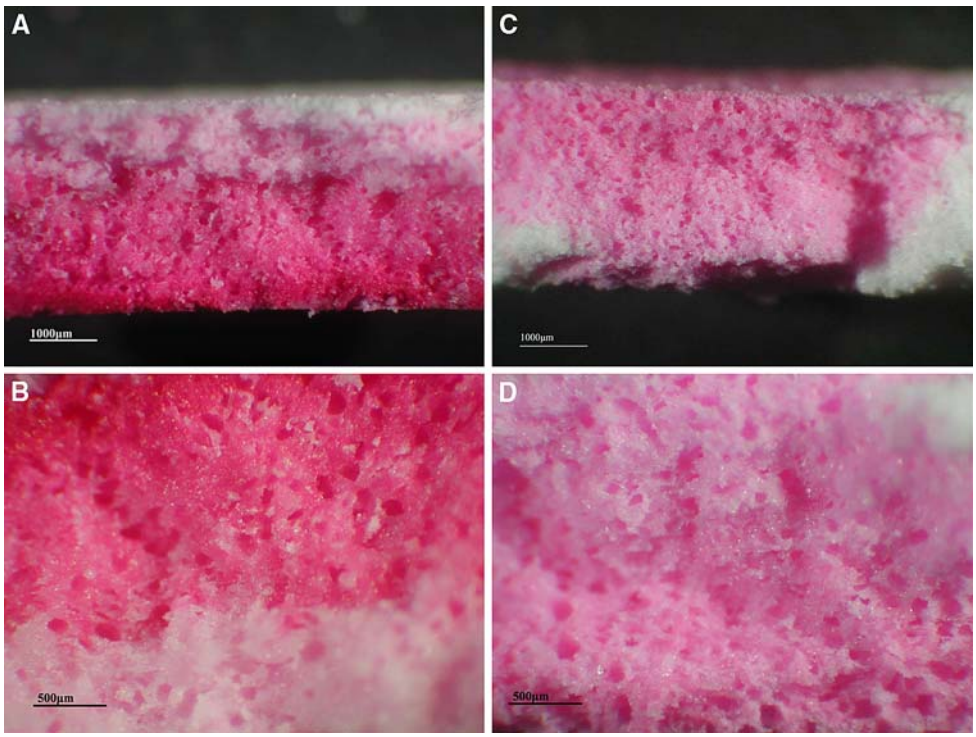

Fig. 2 Cross-section photographs of BG1 and BG2 scaffolds after addition 1% rhodamine dye solution. **a** BG1 complete cross-section, **b** BG1 cross-section higher magnification, **c** BG2 complete cross-section, and **d** BG2 cross-section higher magnification. Note the continuous (*pale pink*) colouring throughout the thickness of BG2, indicating that the porosity was such that the dye readily penetrated through the scaffold structure. (Color figure online)

hydroxycarbonate apatite layer in both scaffold types after SBF immersion [12, 13]. The peak centred approx. 810 cm^{-1} in SBF immersed samples were attributed to C–O stretch vibrations (Fig. 5) (range 890–800 cm^{-1}) were not present in the as-sintered scaffolds [12, 13]. The sharp peaks at approx. 1080 cm^{-1} in both SBF immersed scaffolds relative to the as-sintered scaffolds were associated with an increase in the Si–O–Si stretch vibration (range 1100–1000 cm^{-1}). Peaks observed at approx. 600, 555 and 530 cm^{-1} were each associated with P–O bending vibrations in SBF immersed BG1 scaffolds not present in the as-sintered BG1 scaffold spectra (Fig. 5) (peak ranges of 600–570, 560–550 and 530–515 cm^{-1}, respectively). Similar P–O bending peaks were observed in BG2 SBF immersed scaffolds at approx. 594, 560[1] and 523 cm^{-1} (not shown individually as the FTIR spectra of the immersed scaffolds were very similar for BG1 and BG2). A representative scanning electron micrograph is shown in

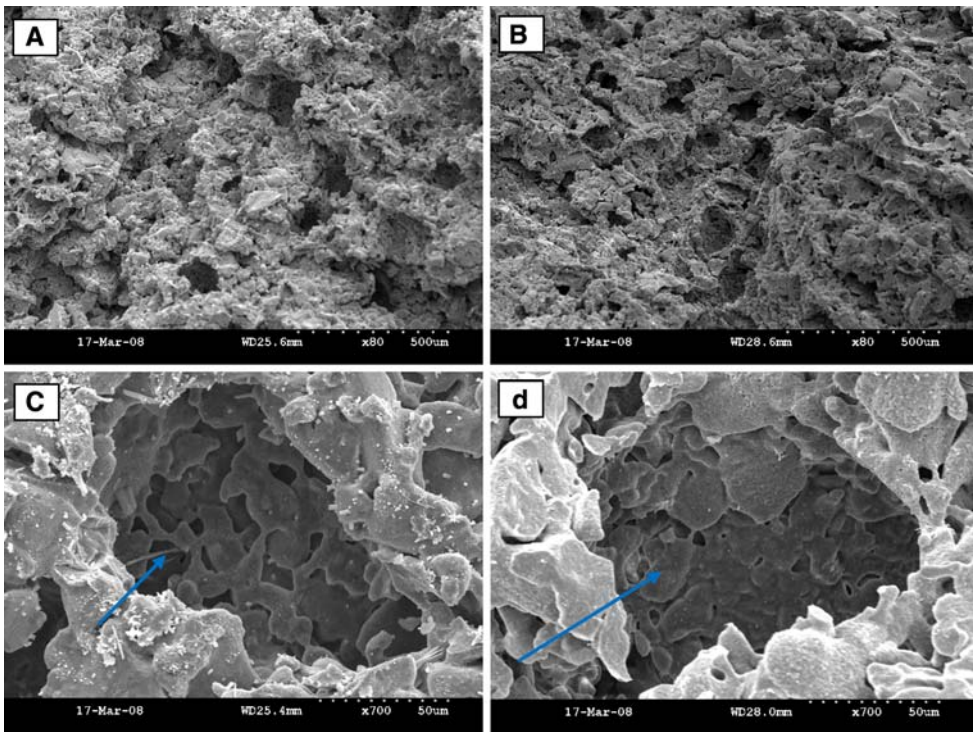

Fig. 3 SEM images of sintered BG1 (**a**) and BG2 (**b**) surface topography of BG1 and BG2, respectively, (×30). **c** and **d** Cross-sectional images of BG1 and BG2 ×700 magnification of a single large pore in BG1 and BG2, respectively, in cross-section. Note the presence of multiple microspores within the single large pore

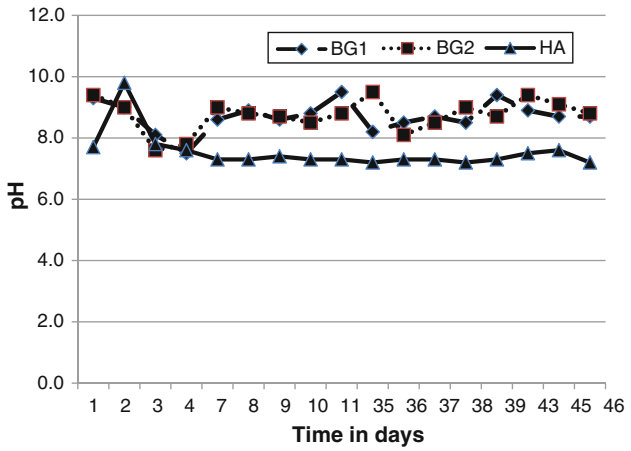

Fig. 4 The variation of pH in SBF immersion medium containing the scaffolds over time

Fig. 6 indicating the appearance of an apatite-like structure.

3.3 In vitro cytocompatibility studies

3.3.1 MTT tests

The results of the MTT assay of the 24 h eluants-24 h exposure, 72 h eluants-24 h exposure and 72 h eluants-72 h exposures of the BG1 and BG2 scaffolds showed little difference between any of the concentrations and the negative controls (HOB medium)—all displaying relatively similar levels of mitochondrial activity and therefore, cell metabolic activity (Figs. 6 and 7). As expected the positive controls were strongly cytotoxic. The graphs in Figs. 6 and 7 clearly show that the eluants were not cytotoxic. Table 1 illustrates the means and 95% confidence intervals of the raw data for BG1 and BG2. Multiple-comparison analysis was performed at each time point comparing each scaffold elution concentration (and the positive control) to the negative control using the non-parametric Kruskal–Wallis analysis at a predetermined 5% level of significance. Differences between the various scaffold elution concentration-exposures and the negative controls were not significant for both scaffold types for both eluant and exposure times (5% level of sig.) (Table 1). Significant differences were only observed between the 50% BG1 eluant dilution at 24 h eluant-24 h exposure and 100% BG1 at 72 h eluant-72 h exposure, the former actually due to a significantly improved response relative to the negative control, whilst the latter, as indicated in Fig. 7, was clearly not far below the negative control and considerably above the positive toxic cell control. Although the statistical analysis compares the negative and positive control in 2D form, they also function as an internal standard whilst the material 3D control used in this study is hydroxyapatite.

3.3.2 Cell proliferation studies

Cell proliferation was assessed at 4, 7, 14, 21 and 28 days, optical densities (equivalent to the degree of cell

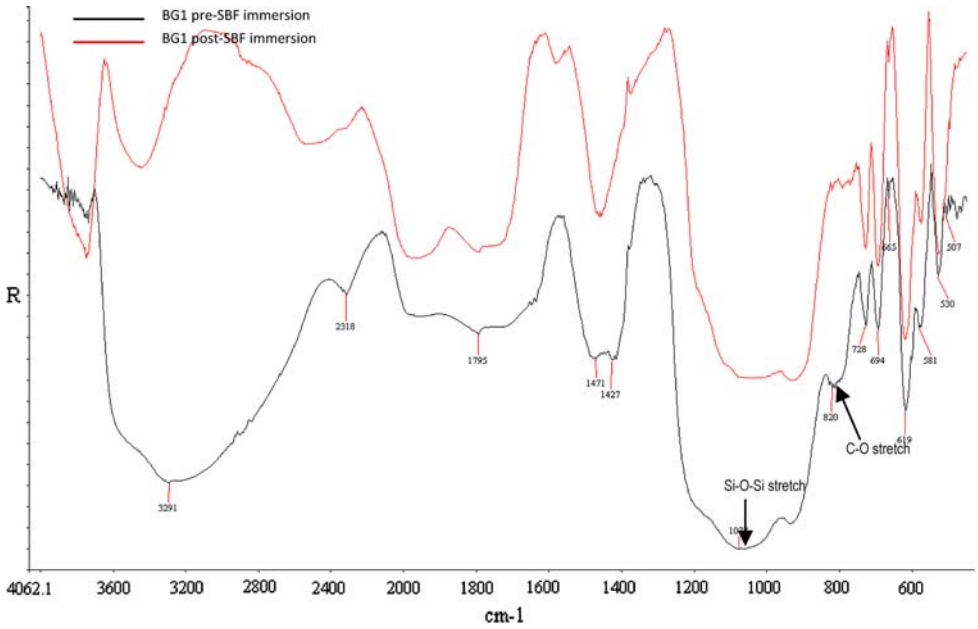

Fig. 5 FTIR of the BG1 scaffold pre and post immersion in simulated body fluid

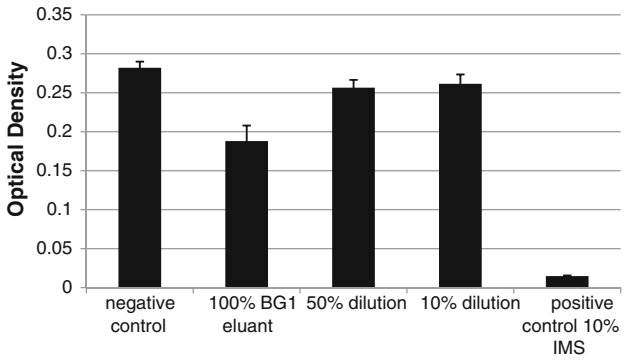

Fig. 6 Mitochondrial activity of HOB cells after 72 h exposure to various dilutions of the 72 h BG1 scaffold elutions as determined by MTT assay

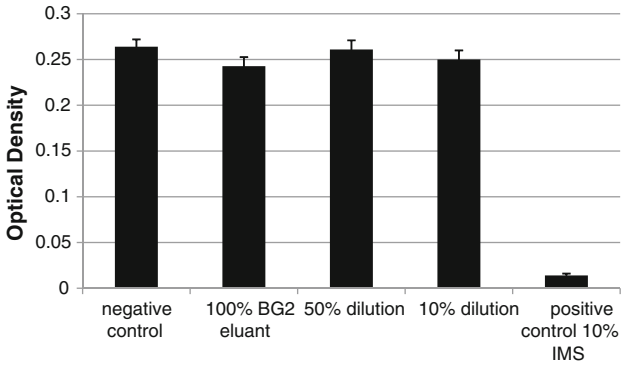

Fig. 7 Mitochondrial activity of HOB cells after 72 h exposure to various dilutions of the 72 h BG2 scaffold elutions as determined by MTT assay

proliferation) recorded for HOB (Table 2) and HUVEC (Table 3) cell-seeded BG1 and BG2 scaffolds were consistently higher than the commercial HA scaffolds. Kruskal–Wallis analysis demonstrated that at all five time points, a significant difference was observed in HOB and HUVEC co-culture proliferation when compared to HA

Table 1 Probabilities in HOB monoculture studies that the differences observed between each eluant-exposure scenario for each scaffold and the negative control were due to chance according to the Kruskal–Wallis multiple comparison analysis with significance pre-determined at $\alpha = 0.05$

	BG1 100% eluant	BG1 50% dilution	BG1 10% dilution	BG2 100% eluant	BG2 50% dilution	BG2 10% dilution
24 h eluant–24 h exposure	0.236645	0.006037	0.075747	0.295339	0.169490	0.154828
	NS	S	NS	NS	NS	NS
72 h eluant–24 h exposure	0.452453	0.337853	0.382544	0.060116	0.018235	0.255470
	NS	NS	NS	NS	NS	NS
72 h eluant–72 h exposure	0.002486	0.084641	0.094297	0.063765	0.440618	0.141029
	S	NS	NS	NS	NS	NS

Note: The adjusted *P*-value for significance = 0.006250. BG1 and BG2 scaffold eluants were analysed separately, each scaffold type having its own negative control. Significant and non-significant differences are marked as **S** and **NS** respectively

Table 2 Probabilities in HOB monoculture studies showed that the differences observed between each scaffold type (as well as positive control) and the negative control were due to chance according to the Kruskal–Wallis multiple comparison analysis with significance pre-determined at $\alpha = 0.05$

	HA	BG1	BG2	+ve Control
Day 4	0.000003	0.016424	0.097722	0.000000
	S	NS	NS	S
Day 7	0.000002	0.011400	0.061216	0.000000
	S	NS	NS	S
Day 14	0.000022	0.015359	0.102424	0.000000
	S	NS	NS	S
Day 21	0.000040	0.019159	0.087368	0.000000
	S	NS	NS	S
Day 28	0.000150	0.006210	0.079164	0.000000
	S	NS	NS	S

Note: The adjusted *P*-value for significance = 0.005. Significant and non-significant differences are marked as S and NS, respectively

Table 3 Probabilities in HUVEC monoculture studies that the differences observed between each scaffold type (as well as positive control) and the negative control were due to chance according to the Kruskal–Wallis multiple comparison analysis with significance pre-determined at $\alpha = 0.05$

	HA	BG1	BG2	+ve Control
Day 4	0.000369	0.044902	0.058042	0.000000
	S	NS	NS	S
Day 7	0.000002	0.034271	0.054012	0.000000
	S	NS	NS	S
Day 14	0.000140	0.016793	0.096190	0.000000
	S	NS	NS	S
Day 21	0.000190	0.027452	0.065659	0.000000
	S	NS	NS	S
Day 28	0.000003	0.083190	0.020445	0.000000
	S	NS	NS	S

Note: The adjusted *P*-value for significance = 0.005. Significant and non-significant differences are marked as S and NS, respectively

relative to the negative control (5% level of sig.). In co-culture, no statistically significant difference was observed between both BG1 and BG2 scaffolds relative to the negative control at all time points, demonstrating that BG1 and BG2 scaffolds exhibited significantly improved HOB and HUVEC cell proliferation in co-culture relative to HA scaffolds (at 5% level of sig.) (Table 4). In HUVECs alone, no statistically significant difference was observed between both BG1 and BG2 scaffolds relative to the negative control for all time points studied, which indicated significantly improved HUVEC cell proliferation in monoculture relative to HA (at 5% level of sig.) (Table 3).

Table 4 Probabilities in HOB and HUVEC co-culture studies that the differences observed between each scaffold type (as well as positive control) and the negative control were due to chance according to the Kruskal–Wallis multiple comparison analysis with significance pre-determined at $\alpha = 0.05$

	HA	BG1	BG2	+ve Control
Day 4	0.000654	0.305401	0.343921	0.000002
	S	NS	NS	S
Day 7	0.000002	0.034271	0.054012	0.000000
	S	NS	NS	S
Day 14	0.000303	0.015707	0.100839	0.000000
	S	NS	NS	S
Day 21	0.000144	0.021342	0.080490	0.000000
	S	NS	NS	S
Day 28	0.000172	0.061216	0.027452	0.000000
	S	NS	NS	S

Note: The adjusted *P*-value for significance = 0.005. Significant and non-significant differences are marked as S and NS, respectively

3.4 HOB and HUVEC co-cultures

Proliferation of co-culture HOB and HUVEC seeded on BG1 and BG2 scaffolds was shown to be higher than the commercial HA scaffolds (Fig. 8; Table 4). Kruskal–Wallis analysis demonstrated that at all five time points, a significant difference was also observed in HOB and HUVEC co-culture proliferation between HA scaffolds relative to the negative control (5% level of sig.). In

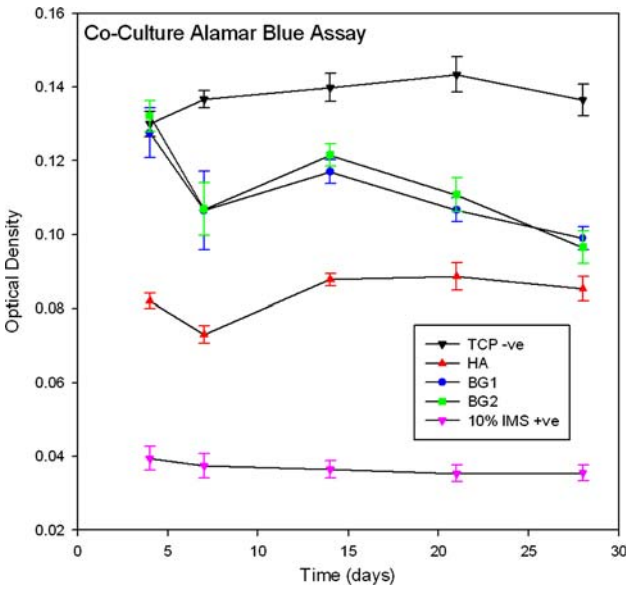

Fig. 8 Combined HOB and HUVEC cell proliferation on cell-seeded scaffolds, positive controls and negative controls across all 5 time points of the alamar Blue™ study. Points correspond to means of the raw data replicates. 95% confidence intervals are included in each case

co-culture, no statistically significant difference was observed between both BG1 and BG2 scaffolds relative to the negative control for all time points studied, thus confirming that BG1 and BG2 scaffolds demonstrated significantly improved HOB and HUVEC cell proliferation in co-culture relative to HA scaffolds (at 5% level of sig.) (Table 4).

Double cytotracker staining of HOBs and HUVECs was performed prior to cell-seeding BG1, BG2 and HA scaffolds in co-culture. Scaffolds were imaged under fluorescence at $\times 10$ magnification using confocal laser scanning microscopy at 4 h, 3 and 6 days post cell-seeding. In all the test scaffolds, fluorescing HOBs and HUVECs could be detected below the surface (i.e. within the porosities of the scaffolds) for all time points studied, since confocal microscopy enabled images of the scaffolds to be taken at various focal planes in the z-axis, typically up to a depth of ≈ 300 μm below the surface of the scaffolds. A representative image of the BG2 scaffold is shown in Fig. 9.

SEM imaging of HOB and HUVEC seeded BG1 and BG2 scaffolds in co-culture was performed in cross-section, the presence of both cell types beneath the outer surface of BG1 and BG2 scaffolds was observed, and a representative image of BG2 scaffold is shown in Fig. 10. SEM confirmed that HOBs and HUVECs were able to penetrate the outer surface of both scaffold types and migrate towards the internal interconnected porous structure. SEM images of BG1 and BG2 cell-seeded scaffolds revealed the presence of various cellular morphologies within the scaffold structures. Flattened cells were observed with stretched morphologies spanning across pores from several attachment points, whilst other cells had numerous filopodia-like extensions or were relatively compact (Fig. 10). Interestingly, deposits were observed on the cellular structures to some degree (Fig. 10) these deposits were thought to be the formation of HCA. Though the images obtained were purely qualitative, they demonstrated that both cell types were able to migrate through the surface of the scaffold types towards the internal porous structure. From a qualitative perspective, the cell density observed in BG1 and BG2 scaffolds also appeared visually greater than that on the HA scaffolds.

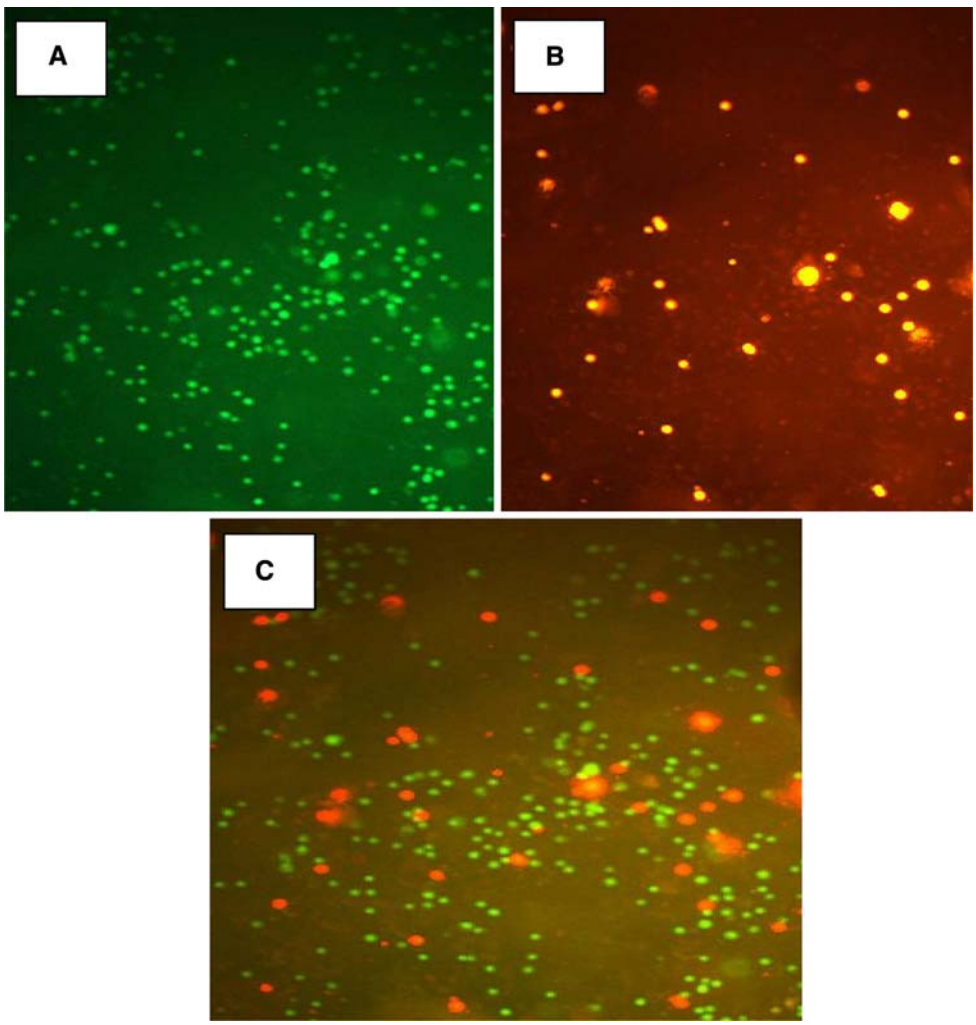

Fig. 9 Cytotracker stained **a** HUVECs (at 492 nm absorbance and 517 nm emission wavelength; *green*) and **b** HOBs (at 548 nm absorbance and 576 nm emission wavelength; *orange*) on a BG2 scaffold at 6 days post seeding at the same focal plane. **c** Overlay of images showing relative positions of both cell types simultaneously. (Color figure online)

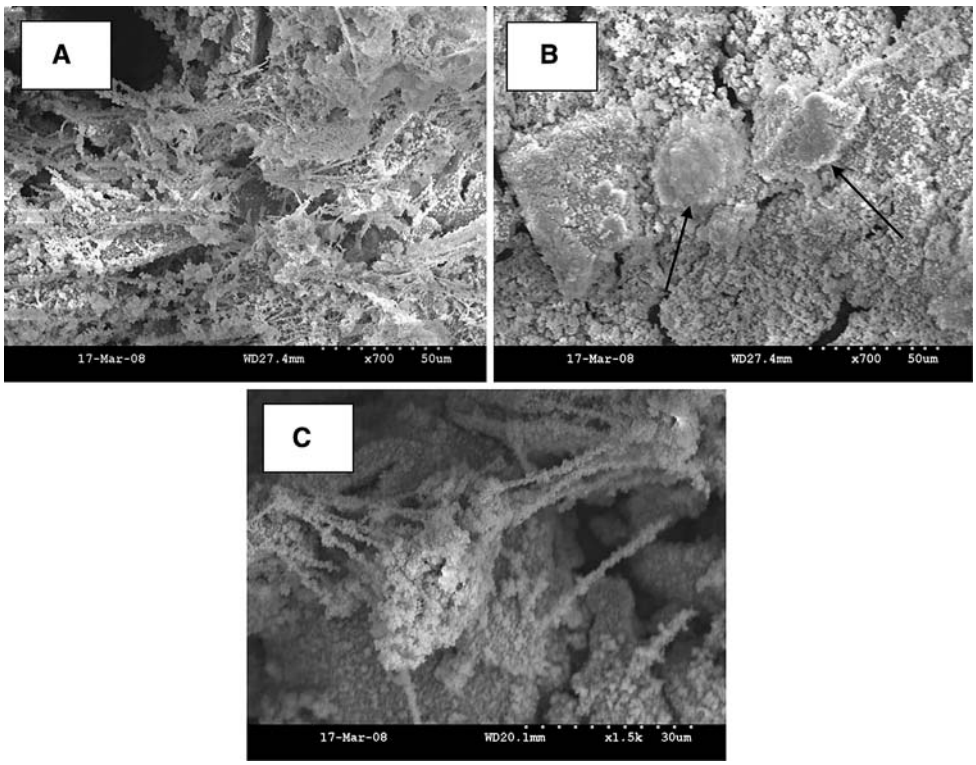

Fig. 10 BG2 scaffolds (**a**, **b** and **c**) in cross-section showing the presence of cells within the interconnected porous structure. Numerous cellular extensions are evident. **b**) Two relatively round HUVECs (*arrowed*) side by side on a BG2 scaffold. Note the presence of apatite formation on the scaffolds as well as the cellular structures mentioned, somewhat obscuring the underlying cellular structures

4 Discussion

Cements or ceramics based on calcium phosphates and bioactive glasses are regarded as the scaffold material of choice due to their osteoconductive properties for bone tissue engineering. One of the problems associated with 3-D scaffolds is the transport of nutrients through the entirety of the scaffold material to support the cells, thus leading to less than required optimal cell–cell interaction. The introduction of porosity is a key to enhancing nutrient flow, however, the failure of tissue-engineered scaffolds is also related to the lack of vascularisation.

Whilst calcium phosphate ceramics clearly demonstrate necessary characteristics such as osteoconductivity and biocompatibility, the additional osteoinductive properties of bioactive glasses, and hence, their potential for much accelerated rates of bone growth within defect sites, sets them firmly apart from other ceramics currently being explored as potential scaffolds [14]. Three dimensional porous scaffolds prepared from 45S5 Bioglass® was selected as the scaffold material due to its bioactive properties and high affinity for cells and was compared with the in vitro performance of commercial SynHApor HA scaffolds (Hi-Por Ceramics Ltd., Sheffield, UK) currently used in bone defect treatment. One of the methods to fabricate porous scaffolds is to use organic materials and eliminate it to yield micro and macroporosity in the scaffold. The porogen used in this study was poly(vinyl alcohol), which was eliminated during the sintering process to create the interconnected porous structure whilst allowing adjacent Bioglass® particles to coalesce to some degree and hence, form a porous construct. Bioactive glass particles are known to crystallize immediately above their glass transition temperature, thus the heat treatment temperature would invariably render the material to be a glass–ceramic and such phase transformation has been known to reduce the level of bioactivity of bioactive glasses. However, the very alkaline nature of Bioglass® dissolution usually leads to damage of cells in contact and the partial conversion to a glass–ceramic is expected to decrease its dissolution properties. The general consensus is that the more soluble the material, the higher the tendency of the apatite deposition and solubility increases with the phases of calcium phosphate present in a matrix [15]. The current study indicated that the scaffolds made from 45S5 Bioglass® although sintered were still bioactive as shown from the in vitro bioactivity tests and the pH of the immersion medium in simulated body fluid was slightly alkaline. 45S5 Bioglass® is a Class A bioactive material, 45S5 Bioglass® that possesses not only osteoconductive properties, but is also osteoinductive—a physiological property typically associated with bone morphogenic proteins (BMPs) (involving stimulation of pluripotent cells to develop into the bone forming lineage), though in terms of synthetic materials, a property that is virtually unique to bioactive glasses. Goller et al. [16] have shown, however, that

sintering of 45S5 Bioglass®-HA composites at 1200°C for 4 h still results in the presence of a considerable glassy phase, suggesting that in the current study, not all of the glass present in BG1 and BG2 had undergone glass–ceramic transformation. Gough et al. [17] have also shown that the temperature at which 45S5 Bioglass® is sintered has a profound impact upon the bioactivity of the subsequent 45S5 Bioglass® derived system, whilst demonstrating that at a sintering temperature of 1000°C, considerable bioactivity is still retained within the Bioglass® derived system.

4.1 In vitro cytotoxicity studies

MTT assay was used to assess the indirect cytotoxicity of BG1 and BG2 scaffold leachables on HOB cells in vitro. The effect of the eluants on cell viability showed no statistically significant differences between any of the eluant-exposure times and their respective negative controls, regardless of eluant concentration (5% level of significance). Only BG1 72 h eluant/72 h exposure at 100% showed a significant reduction in cell response relative to negative control. Thus, suggesting that the increased alkalinity of the eluant as a result of the longer elution time, which is evidenced in the pH of the immersion media may have had an effect. However, this effect in vivo would not cause significant toxicity due to the increased body surface area and clearing system.

4.2 HOB cell proliferation in monoculture

BG1 and BG2 scaffolds performed very favourably in HOB monocultures relative to the commercial HA scaffold control. Cell proliferation in the seeded scaffolds demonstrated good cell response (Fig. 8), with no statistical differences observed between BG1 and BG2 scaffolds (Table 2). An enhanced HOB cell proliferation was observed on both BG1 and BG2 scaffolds relative to HA over the 28 days of study and as both BG1 and BG2 are 45S5 Bioglass® derived, which have already demonstrated a high degree of bioactivity in SBF immersion studies (HCA formation, Fig. 6). Since the bioactivity of bioactive glasses and their glass–ceramic derivatives are known to be considerably greater than HA, this study demonstrated a superior osteoconductivity of BG1 and BG2 relative to the HA scaffold control [18, 19]. Indeed, the dissolution products of 45S5 Bioglass® (namely silica and calcium ions) are known to markedly influence osteoblastic gene-expression, upregulating numerous genes involved in bone homeostasis as well as osteoblast metabolism and proliferation (e.g. the bone mitogenic growth factor IGF-II) [20, 21]. It thus seems reasonable to assume that despite the sintering process, these same dissolution products are likely to be responsible for the improved HOB cell proliferation observed in BG1 and BG2 scaffolds relative to HA. This study confirms the favourable osteoblast response to 45S5 Bioglass® derived glass–ceramics sintered at 1000°C described by other groups [17]. It should be noted however, that the negative and positive controls were both 2D cell systems, hence, their relevance as a means of comparison to the 3D porous BG1 and BG2 scaffold systems is somewhat limited. Thus, the data obtained from 3D HA scaffolds is far more relevant as a means of comparison, where the cell responses of BG1 and BG2 scaffolds were shown to be consistently better than HA control (only shown for BG2 as the images are very similar Figs. 9 and 10; Tables 2, 3 and 4).

4.3 HUVEC proliferation in monoculture

Whilst the general trend of HUVEC proliferation was not as favourable in any of the samples tested when compared to the levels of HOB cell proliferation in monoculture (Figs. 9 and 10), this was largely to be expected, given the fact that endothelial cells are known to exhibit notoriously poor viability when cultured in vitro [6]. In monocultures, endothelial cells typically remain viable for 7–10 days without passage, whilst this figure drops to around 5 days on 3D porous materials without the prior fibronectin coating (typically used in the routine culture of endothelial cells in vitro) [6]. Whilst prior coating with fibronectin has been shown to not only enhance, but in certain circumstances be a prerequisite for endothelial cell attachment to biomaterials, no prior coating of samples with fibronectin was performed in this study, and furthermore, no growth factors were added, such that the response of HUVECs to the unmodified scaffold materials alone could be assessed [22, 23].

An interesting finding was the considerably improved HUVEC response to both BG1 and BG2 scaffolds relative to HA across all five time points of the 28 day study (Fig. 10; Table 3). Indeed, at every time point, the differences in cell proliferation between BG1 and BG2 scaffolds and the negative control was small and statistically insignificant (5% level of sig.) (Table 3). In contrast, for all time points studied the differences between HA scaffold and the negative control were statistically significant (5% level of sig.) (Table 3).

To our knowledge, this study is the first to examine the proliferation of endothelial cells upon bioactive glass derived sintered biomaterials, in the context of a 3D porous scaffold system. To date there is limited literature on the proliferation of endothelial cells on bioactive glasses in vitro, although it has been suggested that bioactive glasses appear to have some form of indirect mitogenic effect upon endothelial cells, though little is known regarding the mechanism of this proposed effect [24].

These previous studies thus, appear to be concordant with the heightened level of HUVEC proliferation observed upon BG1 and BG2 relative to the HA control, suggesting that a common mechanism is responsible for this enhanced endothelial cell proliferation in bioactive glasses and bioactive glass-derived sintered scaffolds. A possible explanation is that the alkaline pH of BG1 and BG2 scaffolds in solution create a favourable pH environment for endothelial cells and may be related to the nature of the dissolution products. Although a correlation was observed between an increase in pH and HUVEC proliferation, whether the actual cause of this improved response to BG1 and BG2 was due to pH, other scaffold dissolution products, scaffold morphology, etc., remains unknown and requires further study.

4.3.1 HOB and HUVEC proliferation in co-culture

Much promise surrounds the concept of co-culturing osteoblast and endothelial cells as a means of potentially addressing the limitations to the clinical application of tissue engineered bone substitutes and in solving problems relating to neovascularisation [6, 25]. Since endothelial cells are the principal cell type involved in physiological neovascularisation processes, it is hoped that their inclusion in bone tissue engineered systems developed in vitro will subsequently increase the rate at which such systems become vascularised in vivo. The challenge of integrating ordered capillary processes into tissue engineered constructs ex-vivo still remains to be addressed. The ultimate goal of such co-culture systems is to develop interconnected microvascular networks within bone tissue engineered systems in vitro by mimicking the physiological principles of vasculogenesis [25]. Ideally, these pre-existing microvascular networks would integrate and form interconnections with the angiogenic response of the host vasculature in vivo, ensuring rapid perfusion of blood to the cells within the scaffold, thus influencing cell viability and growth [26].

As observed in both monoculture cell conditions, the proliferative response of HOB cells and HUVECs in co-culture was significantly improved upon BG1 and BG2 co-culture seeded scaffolds relative to HA over 28 day period (Fig. 8; Table 4). Indeed, the favourable cell response to BG1 and BG2 scaffolds can clearly be seen in Fig. 10 where filopodia-like structures were observed with cells spanning across pores from several attachment points. Such cell morphologies are associated with favourable surfaces for cellular attachment and proliferation.

In this study, no adhesive protein was applied to the scaffold to enhance cell adhesion and no additional growth factors known to have mitogenic effects were used. Cell seeded scaffolds were cultured in the standard culture medium for their respective cell types (an equal mixture of both HOB and HUVEC culture medium in the case of the co-culture studies) in order to assess the response of HOB cells and HUVECs in monocultures and co-culture upon the unmodified scaffolds without augmentation. The improved cell proliferation upon BG1 and BG2 scaffolds relative to the HA control is highly promising. However, it must be mentioned that the self-assembly of cells to form "microcapillary-like structures with central lumen" seen in co-culture studies performed by Unger et al. and Fuchs et al. were not observed in this study upon any of the scaffold biomaterials tested [3, 6], as indicated by the dispersed nature of the HUVECs stained and imaged under fluorescence [Fig. 9].

5 Conclusion

In summary, the scaffolds fabricated from 45S5 Bioglass® demonstrated a porous structure with micro and macroporosity that supported both HOB and HUVEC cells in monoculture and co-culture. This system will be useful in understanding the mechanisms involved in regulating angiogenesis in bone formation and will allow further investigations into the nature of cell–cell interactions for application in tissue engineering.

Acknowledgments The authors acknowledge partial financial support from the Department of Health via the National Institute for Health Research (NIHR) comprehensive Biomedical Research Centre award to Guy's & St Thomas' NHS Foundation Trust in partnership with King's College London.

References

1. Clupper DC, Hench LL. Crystallisation kinetics of tape cast bioactive glass 45S5. J Non-Cryst Solids. 2003;318:43–8.
2. Jones JR, Tsigkou O, Coates EE, Stevens MM, Polak JM, Hench LL. Extracellular matrix formation and mineralization on a phosphate-free porous bioactive glass scaffold using primary human osteoblast (HOB) cells. Biomaterials. 2007;28:1653–63.
3. Fuchs S, Ghanaati S, Orth C, Barbeck M, Kolbe M, Hofmann A, et al. Contribution of outgrowth endothelial cells from human peripheral blood on in vivo vascularization of bone tissue engineered constructs based on starch polycaprolactone scaffolds. Biomaterials. 2009;30:526–34.
4. Santos MI, Tuzlakoglu K, Fuchs S, Gomes ME, Peters K, Unger RE, et al. Endothelial cell colonization and angiogenic potential of combined nano- and micro-fibrous scaffolds for bone tissue engineering. Biomaterials. 2008;29:4306–13.
5. Kirkpatrick CJ, Fuchs S, Hermanns MI, Peters K, Unger RE. Cell culture models of higher complexity in tissue engineering and regenerative medicine. Biomaterials. 2007;28:5193–8.
6. Unger RE, Sartoris A, Peters K, Motta A, Migliaresi C, Kunkel M, et al. Tissue-like self-assembly in cocultures of endothelial cells and osteoblasts and the formation of microcapillary-like structures on three-dimensional porous biomaterials. Biomaterials. 2007;28:3965–76.

7. Kokubo T, Kushitani H, Sakka S, Kitsugi T, Yamamuro T. Solutions able to reproduce in vivo surface-structure changes in bioactive glass ceramic A-W. J Biomed Mater Res. 1990;24:721–34.
8. Di Silvio L, Gurav N. Human cell culture chapter 11. In: Koller MR, Palsson BO, Masters JRW, editors. Human cell culture, vol. 5. Dordrecht: Kluwer Academic Publishers; 2001. p. 221–41.
9. Brien OJ, Wilson I, Orton T, Pognan F. Investigation of the Alamar Blue (resazurin) fluorescent dye for the assessment of mammalian cell toxicity. Eur J Biochem. 2000;267:5421–6.
10. Nakayama GR, Caton MC, Nova MP, Parandoosh Z. Assessment of the Alamar Blue assay for cellular growth and viability in vitro. J Immunol Methods. 1997;204:205–8.
11. Product Information: *Celltracker™ probes for long-term tracing of living cells* (Data sheet code: MP 02925). Molecular Probes™, invitrogen detection technologies (revised: 18 July 2006).
12. Filgueiras MR, La Torre G, Hench LL. Solution effects on the surface reactions of a bioactive glass. J Biomed Mater Res. 1993;27:445–53.
13. Kokubo T, Ito S, Huang ZT, Hayashi T, Sakka S. Ca, P-rich layer formed on high-strength bioactive glass-ceramic A-W. J Biomed Mater Res. 1990;24:331–43.
14. Botchway EA, Dupree MA, Pollack SR, Levine EM, Laurencin CT. Tissue engineered bone: measurement of nutrient transport in three-dimensional matrices. J Biomed Mater Res A. 2003;67: 357–67.
15. Ducheyene P, Qiu Q. Bioactive ceramics: the effect of surface reactivity on bone formation and bone cell function. Biomaterials. 1999;20:2287–303.
16. Goller G, Demirkiran H, Oktar FN, Demirkesen E. Processing and characterization of bioglass reinforced hydroxyapatite composites. Ceram Int. 2003;29:721–4.
17. Gough JE, Clupper DC, Hench LL. Osteoblast responses to tape-cast and sintered bioactive glass ceramics. J Biomed Mater Res. 2004;69:621–8.
18. Jones JR. Bioactive ceramics and glasses. In: Boccaccini AR, Gough J, editors. Tissue engineering using ceramics and polymers. Cambridge: Woodhead Publishing Limited; 2007. p. 52–71.
19. Kirkpatrick CJ, Unger RE, Krump-Konvalinkova V, Peters K, Schmidt H, Kamp G. Experimental approaches to study vascularisation in tissue engineering and biomaterial applications. J Mater Sci: Mater Med. 2003;14:677–81.
20. Xynos ID, Edgar AJ, Buttery LDK, Hench LL, Polak JM. Gene expression profiling of human osteoblasts following treatment with the ionic products of Bioglass® 45S5 dissolution. J Biomed Mater Res. 2001;55:151–7.
21. Hench LL, Xynos ID, Polak JM. Bioactive glasses for in situ tissue regeneration. J Biomater Sci Polym Sci. 2004;15:543–62.
22. Unger RE, Peters K, Wolf M, Motta A, Migliaresi C, Kirkpatrick CJ. Endothelialization of a non-woven silk fibroin net for use in tissue engineering: growth and gene regulation of human endothelial cells. Biomaterials. 2004;25:5137–46.
23. Unger RE, Huang Q, Peters K, Protzer D, Paul D, Kirkpatrick CJ. Growth of human cells on polyethersulfone (PES) hollow fibre membranes. Biomaterials. 2005;26:1877–87.
24. Leach JK, Kaiglar D, Wang Z, Krebsbach PH, Mooney DJ. Coating of VEGF-releasing scaffolds with bioactive glass for angiogenesis and bone regeneration. Biomaterials. 2006;27: 3249–55.
25. Laschke MW, Harder Y, Amon M, Martin I, Farhadi J, Ring A, et al. Angiogenesis in tissue engineering: breathing life into constructed tissue substitutes. Tissue Eng. 2006;12:2093–104.
26. Hunter A, Archer CW, Walker PS, Blunn GW. Attachment and proliferation of osteoblasts and fibroblasts on biomaterials for orthopaedic use. Biomaterials. 1995;16:287–95.